

Highlights

Successful production of Solution Blow Spun YBCO+Ag complex ceramics

AL Pessoa, MJ Raine, DP Hampshire, D K Namburi, J H Durrell, R Zadorosny

- synthesis of precursor solution with YBCO+Ag applicable to solution blow spinning
- production of fabric-like ceramic from sol-gel route
- shrinkage of samples due to Ag-addition

Successful production of Solution Blow Spun YBCO+Ag complex ceramics

AL Pessoa^a, MJ Raine^b, DP Hampshire^b, D K Namburi^c, J H Durrell^c and R Zadorosny^{a,*}

^aSuperconductivity and Advanced Materials Group, São Paulo State University (UNESP) Campus at Ilha Solteira, Brazil

^bSuperconductivity Group, Centre for Materials Physics, Department of Physics, Durham University. DH1 3LE, UK

^cDepartment of Engineering, Trumpington Street, Cambridge CB2 1PZ, UK

ARTICLE INFO

Keywords:

solution blow spinning
silver addition
YBCO
sol-gel
chemical route

ABSTRACT

YBCO fabrics composed of nanowires, produced by solution blow spinning (SBS) are so brittle that the Lorentz force produced by induced currents can be strong enough to damage them. On the other hand, it is known that silver addition improves the mechanical and flux pinning properties of ceramic superconductors. Thus, in this work, we show how we successfully obtained a polymeric precursor solution containing YBCO+Ag salts, which can be spun by the SBS route to produce ceramic samples. Yttrium, barium, copper, and silver metal acetates, and polyvinylpyrrolidone (PVP) (in a ratio of 5:1 wt [PVP:acetates]) were dissolved in a solution with 61.5 wt% of methanol, 12 wt% of propionic acid, and 26.5 wt% of ammonium hydroxide, together with 6 wt% of PVP in solution. Three different amounts of silver (10 wt%, 20 wt%, and 30 wt%) were used in $\text{YBa}_2\text{Cu}_3\text{O}_{7-x}$. The TGA characterizations revealed a lowering of crystallization and partial melting temperatures by about 30 °C. SEM images show that after burning out the polymer, a fabric composed of nanowires of diameters up to 380 nm is produced. However, after the sintering process at 925 °C for 1 h, the nanowires shrink into a porous-like sample.

1. Introduction

The main applications of superconductors are based on devices made by low-temperature materials like NbTi [1] and Nb₃Sn [2]. However, since the discovery of ceramic high-temperature superconductors (HTS), efforts have been made to develop materials and devices with properties and forms specific to each required application. The pros of using HTS in turbines, generators, motors, magnetic shielding, and NMR/MRI are the reduced weight, high efficiency, compact size, low noise, high trapped fields, and so on [3, 4]. On the other hand, the cons of using HTS are their high production cost, high ac-losses, non-homogeneous trapped field distribution, and high cost and reliability of the cooling systems. Some of these issues, however, can be solved by producing materials following facile and low-cost routes and aiming for high values of critical current density J_c and its homogeneous distribution along the length of the materials. Additionally, high porous superconductors, such as those produced by solution-blow spinning (SBS) [5, 6], electrospinning [7, 8], and in foam-like structures [9, 10], could be used to increase cooling efficiency due to their increased surface areas.

Particularly in the case of SBS, the samples have a fabric-like structure formed by network of wires that produces a thin porous material. However, as can be seen by the data in Ref. [11] the samples are very fragile; they are pulverized

during magnetic measurements by the Lorentz force generated by the induced currents in the wires. Therefore, to study their superconducting properties in a wide range of fields and temperatures, it is necessary to improve their mechanical properties.

Research works carried out on bulk (RE)BCO materials, specially in $\text{YBa}_2\text{Cu}_3\text{O}_{7-x}$ (YBCO) system, showed that both the mechanical [12, 13, 14, 15] and superconducting [15, 16, 17] properties could be significantly improved through addition of silver. Some of the other benefits of adding silver is that it does not chemically react with YBCO [17, 18, 19], it improves pinning sites [20], it modifies weak-links [21, 22, 23], and it enhances J_c [18, 24].

A variety of silver composites have been added in YBCO system, such as metallic Ag [18], Ag₂O [12], and AgNO₃ [13, 24]. The samples were usually produced by solid-state reaction [13, 18, 24], melting-growth-like processes [12], and by electrochemical routes [25]. In Ref. [26], a sol-gel chemical route was used to dope the barium site by silver in the production of YBCO pellets. It is reported that high concentrations of silver depreciate the superconducting properties but in small concentrations, it slightly enhances the critical temperature T_c and critical current density J_c . However, as discussed in Ref. [27], there is some controversy as to the extent to which Ag can be doped into YBCO samples. Also, to our best knowledge, there is no information about how the inclusion of silver affects the production process of porous samples using chemical routes, such as in SBS.

The SBS technique was first reported in Ref. [28]. In such a technique, polymer solutions are spun by compressed air from an inner needle up to a collector [28, 29]. Along the working distance i.e. the space between the needle and the collector, the solvents have to evaporate, allowing the for-

*Corresponding author

 alexsanderpessoa@yahoo.com.br (A. Pessoa);

m.j.raine@durham.ac.uk (M. Raine); d.p.hampshire@durham.ac.uk (D. Hampshire); ndevendra@gmail.com (D.K. Namburi); jhd25@cam.ac.uk (J.H. Durrell); rafael.zadorosny@unesp.br (R. Zadorosny)

ORCID(s): 0000-0002-7949-4626 (A. Pessoa); 0000-0001-6566-6039 (M. Raine); 0000-0003-3219-2708 (D.K. Namburi); 0000-0003-0712-3102 (J.H. Durrell); 0000-0002-2419-2049 (R. Zadorosny)

Reagents	Chemical formula	Purity (%)	Brand
Yttrium acetate	$C_6H_9O_{6.5}H_2O$	99.9	Sigma
Barium acetate	$C_4H_6BaO_4$	99	Sigma-Aldrich
Copper acetate	$C_4H_6CuO_4H_2O$	99	Sigma-Aldrich
Silver acetate	$C_2H_3AgO_2$	99	Sigma-Aldrich
Poli(vinylpyrrolidone)*	$(C_6H_9NO)_n$	99.99	Sigma-Aldrich
Propionic acid	$C_3H_6O_2$	99.5	Sigma-Aldrich
Methanol	CH_3OH	99.8	Vetec
Ammonium hydroxide	NH_4OH	PA	Dinamica

*PVP= 1.300.000 g mol⁻¹

Table 1

List of reagents used in the synthesis of precursor solutions.

mation of stretched, thin fibers with diameters of the order of hundreds of nanometers. Thus, solutions with no water (or with very low water content) are crucial to this technique to ensure that the volatility of the solution remains sufficiently high. Apart from some silver composites being easily dissolved in a variety of solvents (including water), the synthesis of a precursor solution with Y, Ba, Cu, and Ag ions is greatly challenging. Here, we describe a sol-gel-based synthesis method for obtaining fabric-like samples using SBS and we present structural characterizations showing the influence of silver content on those properties.

2. Materials and Methods

One-pot-like method [30] was used to synthesize the precursor solution, and the reagents used are shown in Table 1. All salts are heated at 100 °C for about 24 h before being weighed, ensuring that there is no moisture in the salts. This is particularly important as some of these salts are hydrophilic in nature.

2.1. Sol-gel process

The Y, Ba, and Cu acetates were stoichiometrically weighed in the molar ratio 1:2:3, respectively. The Ag acetate was weighed in three concentrations namely 10 wt%, 20 wt%, and 30 wt% with respect to the final mass of ceramic YBCO. Based on the amount of acetates, PVP was weighed in the ratio 5:1 (acetates:PVP). The mass of solvent was set to ensure that the concentration of PVP in solution was 6 wt%. The acetates were placed in a vessel in the specific order Y, Ba, Cu, and Ag, and then propionic acid (12 wt%), methanol (61.5 wt%), and ammonium hydroxide (26.5 wt%) were added. After five minutes of stirring, the PVP was added. The final precursor solution was magnetically stirred for 24 h, with the vessel closed hermetically at room temperature (around 28 °C). Figure 1(a) shows the stabilized YBCO precursor solution and in panel (b) a loaded syringe used in the SBS apparatus. The samples studied in the present work are labeled as YAg0, YAg10, YAg20, and YAg30 with correspondence to the concentration of Ag in YBCO as 0 wt%, 10 wt%, 20 wt%, and 30 wt%, respectively.

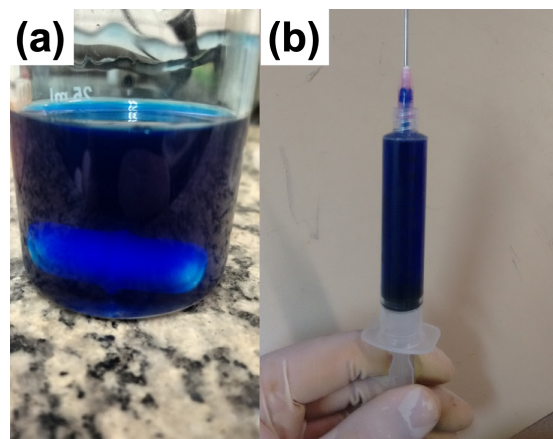


Figure 1: (a) The YAg10 precursor solution. (b) Precursor solution loaded in a 10 ml syringe used in the SBS technique.

2.2. Solution-blow spinning

A 10 ml syringe was connected to a 25G (diameter of 0.5 mm) needle. The air pressure of the compressed air cylinder was adjusted to 1 kPa and the working distance between the needle and the collector was set to 40 cm. The cylindrical collector was rotated at 40 rpm and the solution within the syringe was injected into the compressed gas airflow at a rate of 3 ml h⁻¹. A halogen light was placed above the working distance to locally heat the ejected polymer jet, evaporating the solvents prior to the jet's impact onto the rotating collector.

2.3. Heat-treatments

The as-collected sample was firstly heat-treated at 100 °C for 1 h and then at 150 °C for another 1 h with a heating rate of 5 °C min⁻¹. Some portions of that sample were then used to obtain SEM images. The polymer decomposition was carried out at 600 °C for 3 h ramping the temperature up and down at a rate of 1 °C min⁻¹. Some pieces of the sample at that stage were also used to make SEM analysis. The synthesis was carried out in a tube furnace. The heat-treatment consisted of increasing the temperature from room temperature to 820 °C at 3 °C min⁻¹ and dwelling for 14 h. During the heating process, flowing O₂ was turned on at 500 °C. After that dwell period, the temperature was increased at

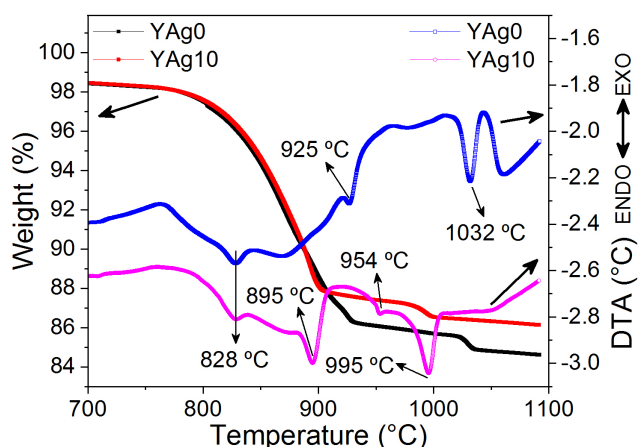


Figure 2: TG and DTA of samples YAg0 and YAg10 carried out after a heat-treatment at 600 °C. The YAg10 lost less mass due to the silver addition. From DTA curves, it is noted that the silver addition shifted the YBCO crystallization peak from 925 °C (YAg0) to 895 °C (YAg10). The partial melting peak is also shifted from 1032 °C for YAg0 to 995 °C for YAg10. The peak at 954 °C is related with the melting of metallic silver.

1 °C min⁻¹ to 925 °C and this was held for 1 h. Then, also at 1 °C min⁻¹, the temperature was decreased to 725 °C for 6 h; then at 3 °C min⁻¹ to 450 °C for 24 h. Finally, the O₂ gas flow was turned off and the temperature was decreased to room temperature at 3 °C min⁻¹.

2.4. Characterizations

Thermogravimetric measurements were carried out on the samples YAg0 and YAg10 (obtained after a heat-treatment at 600 °C), employing TA Instrument, model SDT-Q600. Measurements were carried out under flowing compressed air at a rate of 100 ml min⁻¹ and the temperature was increased from 25 °C to 1000 °C at a rate of 10 °C min⁻¹. For the scanning electron microscopy (SEM) measurements, an EVO LS15 Zeiss operated at 20 kV was used. For that, the samples were attached in an aluminum sample holder with carbon tape, and gold was sputtered on their surface for 2 min (5 nm average thickness) using a QUORUM Model Q150T E. The diameter distribution was measured using a randomly selected set of 100 wires and the free software package ImageJ. The x-ray analysis (XRD) was performed in a Shimadzu XDR-6000 diffractometer with CuK α radiation (wavelength: 1.5418 Å). The displacement ranged from $2\theta = 5^\circ$ to 60° at a scan rate of 1 ° min⁻¹ and measuring in steps of 0.02°.

3. Results and Discussions

Thermal analysis was carried out on two samples YAg0 and YAg10, after both were heat treated at 650 °C. About 15 mg of each sample was used for the measurement and the data obtained is shown in Figure 2. Both the samples exhibited a similar weight loss, as can be seen from the curves in Figure 2. The mass lost between 25 °C and 700 °C (not

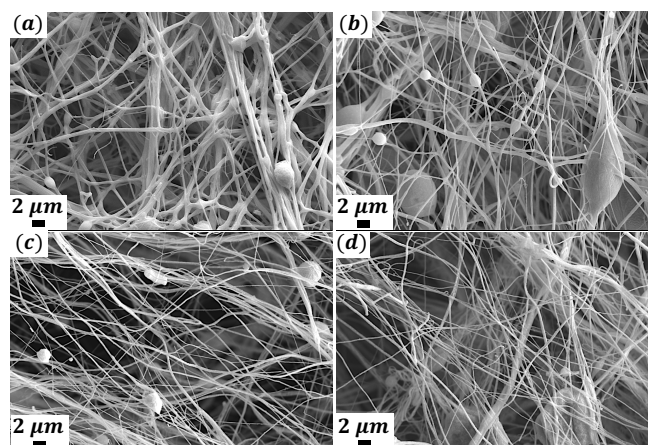


Figure 3: SEM images of samples (a) YAg0, (b) YAg10, (c) YAg20, and (d) YAg30 after calcination at 600 °C. At this step, all samples have the fabric-like morphology with beads distributed along their lengths.

shown in Figure 2), was 1.5 %, and can be associated to the evaporation of water adsorbed in the surface of the samples from the atmosphere or even some organic groups remaining after the heat-treatment. It is also observed that YAg10 lost about 1.1% less mass than YAg0 due to silver addition. It is not shown here, but it is worth pointing out that the PVP degradation occurs between 400 °C and 550 °C [8, 31, 32].

The DTA curves of YAg0 and YAg10 are quite distinct. Both samples present an endothermic peak at 828 °C which can be associated with the reaction between Y₂Cu₂O₅ and BaCuO₂ forming YBCO [33, 34]. The endothermic peak at 925 °C for YAg0 can be associated with the YBCO crystallization, and it was the temperature chosen to be applied in all samples presented in this study. However, it can be noted that the YBCO begins to crystallize at about 895 °C for YAg10, which means that the silver addition reduced the the crystallization temperature by 30 °C (or 3%). The peak at 954 °C presented by YAg10 is associated with the melting of metallic silver [35]. On the other hand, the endothermic peak at 1031 °C for YAg0 is due to a partial melting of YBCO and such a peak is shifted to 995 °C (or 3.5%) for YAg10, showing that the silver addition also decreases this temperature [14, 36, 37].

Based on the thermogravimetric analysis of Figure 2 and on the literature [5, 8, 31, 32], the samples were firstly heat-treated at 600 °C to ensure the total decomposition of the PVP. Figure 3 shows SEM images of the produced samples. All of which present a fabric-like structure with randomly entangled wires, however, it can be seen that beads are distributed along those wires. This is probably due to water from the acid–base reaction in the precursor solution synthesis. Besides that, the wires are long and smooth. Table 2 shows the average diameter (d_{av}) of the samples. Wires in the size range 180 nm to 233 nm were found in the samples. No clear relationship was found between d_{av} and the content of silver present in the system.

Sample	d_{av} (nm)	Deviation (nm)
YAg0	233	77
YAg10	180	68
YAg20	206	76
YAg30	191	63

Table 2

Average diameters of the samples heat-treated at 600° with their respective deviations.

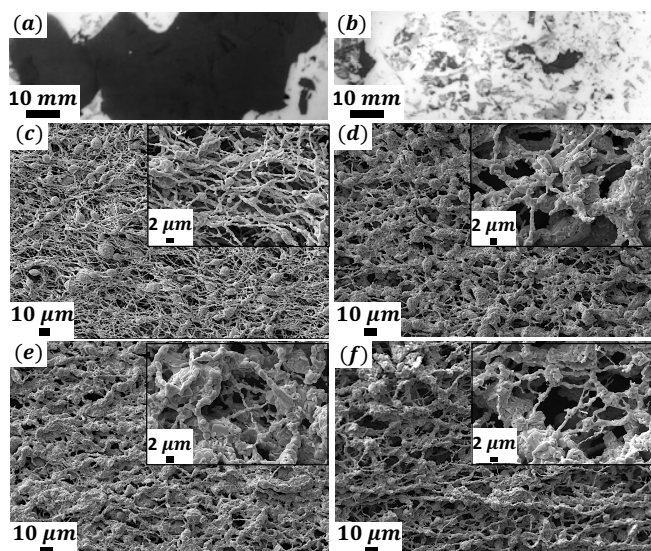


Figure 4: (a) Image of the YBCO-Ag after heat-treatment at 600°C, and panel (b) shows the visible shrinkage of the sample after sintering at 925°C. (c) SEM images of YAg0 sample showing the formation of the wires network structure. From (d) to (f) are the SEM images of the YAg10, YAg20, and YAg30, respectively, showing a porous-like structure due to shrinkage after the sintering process.

After the sintering process at 925 °C, the silver samples shrank, producing a granular porous-like structure. The shrinkage of the samples is shown in Figure 4 (a) and (b). The scale bars within those images are an approximation for comparison purposes. Figure 4(c) shows that, while the Ag-free sample YAg0 maintains its fiber-like structure, the Ag-added samples showed considerable enhancement in density, as shown in Figure 4 from panels (d) to (f). With the wires closer to each other, the grains begin to coalesce during the sintering process and the samples acquire a porous-like morphology. Some works report that the heat-treatment temperatures can be reduced with Ag addition in YBCO bulks [14, 36, 37] due to enhanced heat diffusion. In the case of the present work, the presence of Ag facilitates improved heat-diffusion between the ceramic grains, decreasing the sintering temperature of the samples.

Figure 5 shows XRD diffractograms of all the samples currently studied where it can be seen that the BaCuO₂ phase is present within each of them. Since samples that were produced using PVP of 360.000 g mol⁻¹ instead of 1300.000 g mol⁻¹

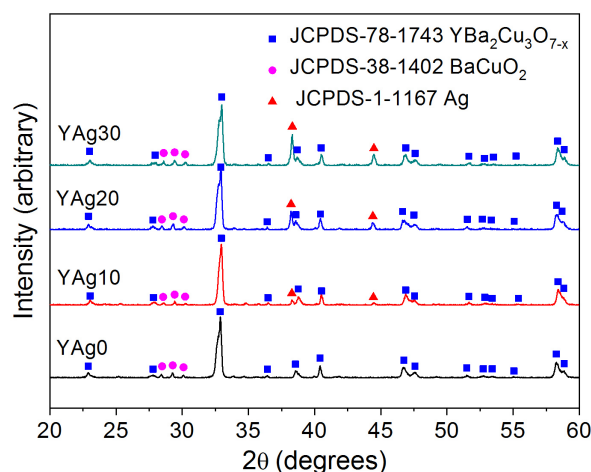


Figure 5: XRD diffractograms of the produced samples. It can be seen that BaCuO₂ is present in all the samples. The main YBCO peak is at $2\theta = 32.88^\circ$, 32.96° , 32.92° , and 32.98° , for YAg0, YAg10, YAg20, and YAg30, respectively. The metallic silver peaks are those ones at 38.28° and 44.5° for YAg10, 38.22° and 44.4° for YAg20, and 38.3° and 44.48° for YAg30.

contain a pure phase [5], we believe that a longer polymer chain could influence the ceramic phase formation. Such a study will be published in future. As the silver content increases, the intensity of the silver peaks (at around 38° and 49°) also increases. The most intense YBCO peak position shifts with the silver addition, being at $2\theta = 32.88^\circ$, 32.96° , 32.92° , and 32.98° , for YAg0, YAg10, YAg20, and YAg30, respectively. This can indicate that there is some saturation for silver doping above which metallic silver begins to form along the sample [27]. The peaks around $2\theta = 38.3^\circ$ and 44.5° were identified as characteristic of metallic silver, and their intensity increases with increasing Ag content.

4. Conclusions

In the present work we report the synthesis of YBCO-Ag nanowires via solution blow spinning SBS technique. This approach is based on an acetate chemical route where yttrium, barium, copper and silver acetates were dissolved in a solution with propionic acid (12 wt%), methanol (61.5 wt%), and ammonium hydroxide (26.5 wt%). The silver was added in amounts of 10 wt%, 20 wt%, and 30 wt%. Thermogravimetric analysis show that the addition of silver decreases both the YBCO crystallization and the partial melting temperatures by 30 °C. Both DTA and XRD characterizations showed the presence of metallic silver. Another interesting influence of silver in such complex ceramics is the huge densification of the samples sintered at 925 °C for one hour. SEM images show that the fabric-like morphology of the samples heat-treated at 600 °C is lost with the sintering process, for which a porous-like morphology takes place due to a shrinkage of the ceramic wire network. Thus, the routine described in this study could be used to produce high density bulk superconductors for use in applications such as flywheels, trapped magnets, motors and generators.

5. Acknowledgements

A. L. Pessoa, R. Zadorosny, M. Raine and D. P. Hampshire acknowledge the Brazilian agencies São Paulo Research Foundation (FAPESP, grant 2017/50382-8), Coordenação de Aperfeiçoamento de Pessoal de Nível Superior (CAPES) – Finance Code 001, and National Council of Scientific and Technologic Development (CNPq, grant 302564/2018-7). We also thanks Prof. Agda E. S. Albas and Silvio R. Teixeira, from UNESP-Presidente Prudente, for the thermogravimetric measurements.

References

- [1] K. M. Schaubel, A. R. Langhorn, W. P. Crendon, N. W. Johanson, S. Sheynin, R. J. Thome, Development of a superconducting magnet system for the ONR/GA homopolar motor, AIP Conf. Proc. 823 (2006) 1819, DOI: 10.1063/1.2202611
- [2] K. S. Haran, D. Loder, T. O. Deppen, L. Zheng, Actively shielded, high field air-core superconducting machines, IEEE Trans. Appl. Supercond. 26 (2016) 98–105. DOI: 10.1109/TASC.2016.2519409
- [3] K. S. Haran, S. Kalsi, T. Arndt, H. Karmaker, R. Badcock, B. Buckley, T. Haugan, M. Izumi, D. Loder, J. W. Bray, P. Masson, E. W. Stautner, High power density superconducting rotating machines-development status and technology roadmap, Supercond. Sci. Technol. 30 (2017) 123002. DOI: 10.1088/1361-6668/aa833e
- [4] J. H. Durrell, M. D. Ainslie, D. Zhou, P. Vanderbenden, T. Bradshaw, S. Speller, M. Filipenko, and D. A. Cardwell, Bulk superconductors: a roadmap to applications, Supercond. Sci. Technol. 31 (2018) 103501. DOI: 10.1088/1361-6668/aad7ce
- [5] M. Rotta, L. Zadorosny, C. L. Carvalho, J. A. Malmonge, L. F. Malmonge, R. Zadorosny, YBCO ceramic nanofibers obtained by the new technique of solution blow spinning, Ceramics International 42 (2016) 16230–16234. DOI: 10.1016/j.ceramint.2016.07.152
- [6] M. Rotta, M. Motta, A. L. Pessoa, C. L. Carvalho, W. A. Ortiz, R. Zadorosny, Solution blow spinning control of morphology and production rate of complex superconducting $YBa_2Cu_3O_{7-x}$ nanowires, Journal of Materials Science: Materials in Electronics 30 (2019) 9045–9050. DOI: 10.1007/s10854-019-01236-w
- [7] X. L. Zeng, M. R. Koblishka, T. Karwoth, T. Hauet, U. Hartmann, Preparation of granular Bi-2212 nanowires by electrospinning, Supercond. Sci. Technol. 30 (2017) 035014. DOI: 10.1088/1361-6668/aa544a
- [8] Z. Shen, Y. Wang, W. Chen, L. Fei, K. Li, H. L. W. Chan, L. Bing, Electrospinning preparation and high-temperature superconductivity of $YBa_2Cu_3O_{7-x}$ nanotubes, Journal of Materials Science 48 (2013) 3985–3990. DOI: 10.1007/s10853-013-7207-y
- [9] E. S. Reddy, G. J. Schmitz, Superconducting foams, Supercond. Sci. Technol. 15 (2002) L21–L24. DOI: 10.1088/0953-2048/15/8/101
- [10] M. R. Koblishka, S. P. K. Naik, A. Koblishka-Veneva, M. Murakami, D. Gokhfeld, E. S. Reddy, G. J. Schmitz, Superconducting YBCO Foams as Trapped Field Magnets. Preprints 2019, 2019010174 (doi: 10.20944/preprints201901.0174.v1).
- [11] Data showing non-reproducibility measurements of fabric-like YBCO samples due to its pulverization by the induced Lorentz force in the brittle wires, <https://dx.doi.org/10.15128/r2f1881k89x> and associated materials are on the Durham Research Online website: <http://dro.dur.ac.uk/>
- [12] P. Diko, G. Fuchs, G. Krabbes, Influence of silver addition on cracking in melt-grown YBCO, Physica C: Superconductivity and its Applications 363 (2001) 60–66. DOI: 10.1016/S0921-4534(01)00622-0
- [13] E. Mogilko, Y. Schlesinger, The $AgNO_3$ route to the YBCO/Ag composite: Structural and electrical properties, Supercond. Sci. Technol. 10 (1997) 134–141. DOI: 10.1088/0953-2048/10/3/003
- [14] J. V. J. Congreve, Y. Shi, K. Y. Huang, A. R. Dennis, J. H. Durrell, D. A. Cardwell, Improving Mechanical Strength of YBCO Bulk Superconductors by Addition of Ag, IEEE Transactions on Applied Superconductivity 29 (2019) 6802305. DOI: 10.1109/TASC.2019.2907474
- [15] P. D. Azambuja, P. R. Júnior, A. R. Jurelo, F. C. Serbena, C. E. Foerster, R. M. Costa, G. B. Souza, C. M. Lepienski, A. L. Chinelatto, Effects of Ag addition on some physical properties of granular $YBa_2Cu_3O_{7-\delta}$ superconductor, Braz. J. Phys. 39 (2009), pp. 638–644. DOI: 10.1590/S0103-97332009000600005
- [16] B. A. Malik, M. A. Malik, K. Asokan, Magneto transport study of YBCO: Ag composites, Current Applied Physics 16 (2016) 1270–1276. DOI: 10.1016/j.cap.2016.07.004
- [17] N. D. Kumar, P. M. S. Raju, S. P. K. Naik, T. Rajasekharan, V. Seshubai, Effect of Ag addition on the microstructures and superconducting properties of bulk YBCO fabricated by directionally solidified preform optimized infiltration growth process, Physica C: Superconductivity and its Applications 496 (2014) 18–22. DOI: 10.1016/j.physc.2013.06.013
- [18] B. A. Malik, M. A. Malik, K. Asokan, Enhancement of the critical current density in YBCO/Ag composites, Chinese Journal of Physics 55 (2017) 170–175. DOI: 10.1016/j.cjph.2016.10.015
- [19] H. Azhan, F. Fariesha, S. Y. S. Yusainee, K. Azman, S. Khalida, Superconducting properties of Ag and Sb substitution on low-density $YBa_2Cu_3O_8$ superconductor, Journal of Superconductivity and Novel Magnetism 26 (2013) 931–935. DOI: 10.1007/s10948-012-2020-4
- [20] S. V. Pysarenko, A. V. Pan, S. X. Dou, Influence of Ag-doping and thickness on superconducting properties of $YBa_2Cu_3O_7$ films, Physica C: Superconductivity 460 (2007) 1363–1364. DOI: 10.1016/j.physc.2007.04.175
- [21] H. Salamati, A. A. Babaei-Brojeny, M. Safa, Investigation of weak links and the role of silver addition on YBCO superconductors, Supercond. Sci. Technol. 14 (2001) 816–819. DOI: 10.1088/0953-2048/14/10/302
- [22] P. Rani, A. Pal, V. P. S. Awana, High field magneto-transport study of $YBa_2Cu_3O_{7-x}Ag_x$ ($x = 0.00 - 0.20$), Physica C: Superconductivity and its Applications 497 (2014) 19–23. DOI: 10.1016/j.physc.2013.10.008
- [23] M. Tepe, I. Avcı, H. Kocoglu, D. Abukay, Investigation of the variation in weak-link profile of $YBa_2Cu_{3-x}Ag_xO_{7-\delta}$ superconductors by Ag doping concentration, Solid State Communications 131 (2004) 319–323. DOI: 10.1016/j.ssc.2004.05.015
- [24] M. Farbod, M. R. Batvandi, Doping effect of Ag nanoparticles on critical current of $YBa_2Cu_3O_{7-\delta}$ bulk superconductor, Physica C: Superconductivity and its Applications 471 (2011) 112–117. DOI: 10.1016/j.physc.2010.11.005
- [25] S. Reich, I. Felner, Nonrandom ceramic superconductor-metal composites, Journal of Applied Physics 67 (1990) 388–392. DOI: 10.1063/1.345267
- [26] F. F. Ramli, N. A. Wahab, A. Hashim, Microstructure and superconducting properties of Ag-substituted $YBa_{2-x}Ag_xCu_3O_{7-\delta}$ ceramics prepared by sol-gel method, MJFAS Malaysian Journal of Fundamental and applied sciences 13 (2017) 82–85. DOI: 10.11113/mjfas.v13n2.655
- [27] J. M. S. Skakle, Crystal chemical substitutions and doping of $YBa_2Cu_3O_x$ and related superconductors, Materials Science and Engineering R23 (1998) 1–40. DOI: 10.1016/S0927-796X(98)00010-2
- [28] E. S. Medeiros, G. M. Glenn, A. P. Klamczynski, W. J. Orts, L. H. C. Mattoso, Solution blow spinning: a new method to produce micro- and nanofibers from polymer solutions, J. Appl. Polym. Sci. 113 (2009) 2322–2330. DOI: 10.1002/app.30275
- [29] J. L. Daristotle, A. M. Behrens, A. D. Sandler, P. Kofinas, A review of the fundamental principles and applications of solution blow spinning, Appl. Mater. Interfaces 8 (2016) 34951–34963. DOI: 10.1021/acsami.6b12994
- [30] M. Rotta, M. Motta, A. L. Pessoa, C. L. Carvalho, C. V. Deimling, P. N. Lisboa-Filho, W. A. Ortiz, R. Zadorosny, One-pot-like facile synthesis of $YBa_2Cu_3O_{7-\delta}$ superconducting ceramic: Using PVP to obtain a precursor solution in two steps, Materials Chemistry and Physics 243 (2020) 122607. DOI: 10.1016/j.mater.chem.phys.2020.122607

- 10.1016/j.matchemphys.2019.122607
- [31] J. Yuh, L. Perez, W. M. Sigmund, J. C. Nino, Sol-gel based synthesis of complex oxide nanofibers, *J.Sol-GelSci. Technol.* 42 (2007) 323–329. DOI: 10.1007/s10971-007-0736-6
 - [32] E. A. Duarte, N. G. Rudawski, P. A. Quintero, M. W. Meisel, J. C. Nino, Electrospinning of superconducting YBCO nanowires, *Supercond. Sci. Technol.* 28 (2014) 015006–015012. DOI: 10.1088/0953-2048/28/1/015006
 - [33] L. C. Pathak, S. K. Mishra, A review on the synthesis of Y–Ba–Cu–oxide powder, *Supercond. Sci. Technol.* 18 (2005) R67–R89. DOI: 10.1088/0953-2048/18/9/R01
 - [34] N. A. Kalanda, V. M. Trukhan, S. F. Marenkin, Phase Transformations in the $Y_2Cu_2O_5$ –BaCuO₂ System, *Inorganic Materials* 38 (2002) 494–497.
 - [35] S. Kohayashi, S. Yoshizawa, H. Miyairi, H. Nakane, S. Nagaya, Large domain growth of Ag–doped YBaCuO–system superconductor, *Materials Science and Engineering: B* 53 (1998) 70–74. DOI: 10.1016/S0921-5107(97)00304-8
 - [36] Y. Nakamura, K. Tachibana, H. Fujimoto, Dispersion of silver in the melt grown $YBa_2Cu_3O_{6+x}$ crystal, *Physica C* 306 (1998) 259–270. DOI: 10.1016/S0921-4534(98)00368-2
 - [37] C. Cai, K. Tachibana, H. Fujimoto, Study on single-domain growth of $Y_{1.8}Ba_{2.4}Cu_{3.4}O_y/Ag$ system by using Nd_{123}/MgO thin film as seed, *Supercond. Sci. Technol.* 13 (2000) 698–702. DOI: 10.1088/0953-2048/13/6/314